Int. J. Electrochem. Sci., 11 **(2016)** 3024 - 3038

International Journal of
ELECTROCHEMICAL
SCIENCE
www.electrochemsci.org

The Inhibition Effect of Polyaspartic Acid and Its Mixed Inhibitor on Mild Steel Corrosion in Seawater Wet/Dry Cyclic Conditions

Xiumin Ma[1,*], *Bei Qian*[2], *jie zhang*[1], *Weichen Xu*[1], *Quantong Jiang*[1], *Meng Zheng*[1], *Fubin Ma*[1], *Baorong Hou*[1]

[1] Institute of Oceanology, Chinese Academy of Sciences, 7 Nanhai Road, Qingdao 266071, PR China
[2] Qingdao Agricultural University, Qingdao 266109, China
[*]E-mail: xma@qdio.ac.cn

Received: 7 December 2015 / *Accepted:* 8 February 2015 / *Published:* 1 March 2015

The inhibition effects of polyaspartic acid (PASP) and the mixed inhibitor (50mg/L PASP, 100mg/L Na_2WO_4, 100mg/L $ZnSO_4.7H_2O$) on mild steel corrosion in seawater wet/dry cyclic conditions were studied via weight loss and electrochemical methods. The polarization curves show that the inhibition efficiency is 72.4% in the presence of PASP, and rises up to 92.6% after the addition of the mixted inhibitor. Scanning electron microscopy (SEM), X-ray diffraction and Fourier transform infrared reflection were performed to study the corrosion inhibition effect. According to the results of SEM, the metal surface immersed in the mixed inhibitor was better protected than that in PASP due to the formation of a protective film.

Keywords: Mild steel, EIS, SEM, XRD, Neutral inhibition

1. INTRODUCTION

There are many different approaches to protect metals against harsh corrosion environments. The most important one is to use corrosion inhibitors [1]. For metals served in marine environments, one of the most widely used strategies is to employ organic compounds as inhibitors. [2-6]. Most of the effective organic inhibitors contain heteroatom such as N,O,S, and multiple bonds in their molecules through which they can adsorb on metal surface [7–10]. As a new type of corrosion inhibitor, the use of polymers has attracted wide attention in recent years [2, 11-16]. Moreover, with the increasing awareness of environmental protection, the development of non-toxic inhibitors has become a hot topic. PASP is an eco-friendly and biodegradable anionic polypeptide, which is widely used as an effective dispersant and antiscalant in paint and paper processing, biomedical applications, and water

treatment [17]. It can be synthesized either by thermal polymerization of aspartic acid monomer with or without catalyst or by hydrolysis of polysuccinimide (PSI) [18,19]. PASP was used as corrosion inhibitor to protect carbon steel in the previous work [20].

In many cases, synergism between inhibitors could play better anticorrosive effects [21]. The previous studies show that the synergism effect of PASP with zinc and wolfram ions revealed good corrosion inhibition effect [22-23]. Most of them focused on the study of corrosion inhibition behavior performance of PASP and the mixed inhibitor containing PASP under full immersion conditions, but none of them have tried it under wet/dry cyclic conditions.

Previous work of the authors studied the anticorrosive effect of PASP with I^- on mild steel in acid solution [3]. The present work focus on the corrosion inhibition behavior of PASP with zinc and wolfram ions on mild steel under wet/dry cyclic conditions. Electrochemical impedance spectra (EIS), polarization, SEM, Fourier transform infrared reflection (FTIR), and X-ray diffraction (XRD) methods were used to investigate the inhibition effect of PASP and the mixed inhibitor under wet/dry cyclic conditions.

2. EXPERIMENTAL

2.1. Materials and solutions

The composition (wt.%) of the mild steel tested in this work was 0.16 C, 0.53 Mn, 0.30 Si, <0.045 P, <0.055 S, and Fe balance. The method for synthesizing the polyaspartic acid has already been described in the previous work of the authors [3].Three kinds of solutions were used: blank sample solutions, 1g/L polyaspartic acid-containing seawater and the mixed inhibitor containing 50mg/L polyaspartic acid, 100mg/L Na_2WO_4, 100mg/L $ZnSO_4.7H_2O$.

2.2. Wet/dry cyclic corrosion tests

All the samples used for electrochemical experiments were immersed in and taken out of the test solution without rotation by an electric screw rod. The solution tank was kept in a thermostatic and humidistatic chamber. In this work, one wet/dry cycle indicates immersing the sample in seawater with or without inhibitors for 8 h, then taking it out and drying at 298 K and 50% humidity for 16 h. X cycles means repeating the cycle for x times. The solution was replaced after each cycle for eight cycles in total.

2.3. Electrochemical measurements

For electrochemical experiments, the specimens were embedded in epoxy resin with an exposed area of 1 cm^2. Seawater from Huiquan Bay in Qingdao was used as the test solution, which was filtered before the test. Prior to all measurements, the samples were abraded with emery paper from 400 to 1200 grit, and then degreased ultrasonically in ethanol and acetone, and dried at room temperature. All electrochemical measurements were performed in a conventional three-electrode cell

with a platinum counter electrode and a saturated calomel electrode coupled to a fine Luggin capillary as the reference at 298 K and repeated three times using the PARSTAT 2273 advanced electrochemical system (Princeton Applied Research). EIS was carried out at open circuit potential (OCP) in the frequency range of 10 mHz–100 kHz with AC signals of amplitude 10 mV and the immersion times were 0.5 h, 2 h, 8h, 2 cycles, 4 cycles, 6 cycles, 8 cycles, respectively. The polarization curves were obtained with a 1 mV/s scan rate and started from a potential of -250 mV to 250 mV vs. OCP after the 8 wet/dry cycles.

2.4. Corrosion product analysis

The surface morphology of the specimens after wet/dry cycles in seawater containing PASP or the mixed inhibitor was observed using the SEM JEOL-JSM-5600. The corrosion products were scraped off from the corroded samples using a razor blade, and were characterized by FTIR and XRD. FTIR spectroscopy was performed using the Bruker Vertex 70 FTIR. Spectra were collected from 16 scans at a resolution of 4 cm^{-1} between 400 cm^{-1} and 4000 cm^{-1}. XRD was performed using the Rigaku-D/max2500PC, with a Cu anode operating at 40 kV, 10–55° scan range, and 5°/min scan speed.

3. RESULTS AND DISCUSSION

3.1. Electrochemical studies

3.1.1. Electrochemical impedance spectroscopy

Fig.1 shows the Nyquist and Bode plots of the mild steel in seawater with 1g/L PASP. Equivalent circuit as depicted in Fig. 2 was used to simulate the impedance data in Fig. 1. The Nyquist plot shows that the radius of capacitive circle increases with immersion time, indicating that more and more PASP molecules are adsorbed on the active sites of steel surface, which inhibits the charge transfer reaction. Meanwhile, the Warburg impedance at low frequency disappeared gradually after 8 h immersion. The results reflect that oxygen and nitrogen atoms in PASP structure cover the metal surface by adsorption or coordination preventing the diffusion process of corrosion products and dissolved oxygen. The corresponding electrochemical parameters are given in Table 1. The R_{ct} value of the sample in seawater without PASP has been reported to be 1963 Ω cm^2 in our previous study [2], and the R_{ct} value is 1815 Ω cm^2 in the seawater with 1g/L PASP solutions after 2h immersion and 3619 Ω cm^2 after 8 h immersion in this work (see Table1), indicating that the formation of the protective film is very slow and the PASP itself does not have a good inhibition effect on mild steel in seawater.

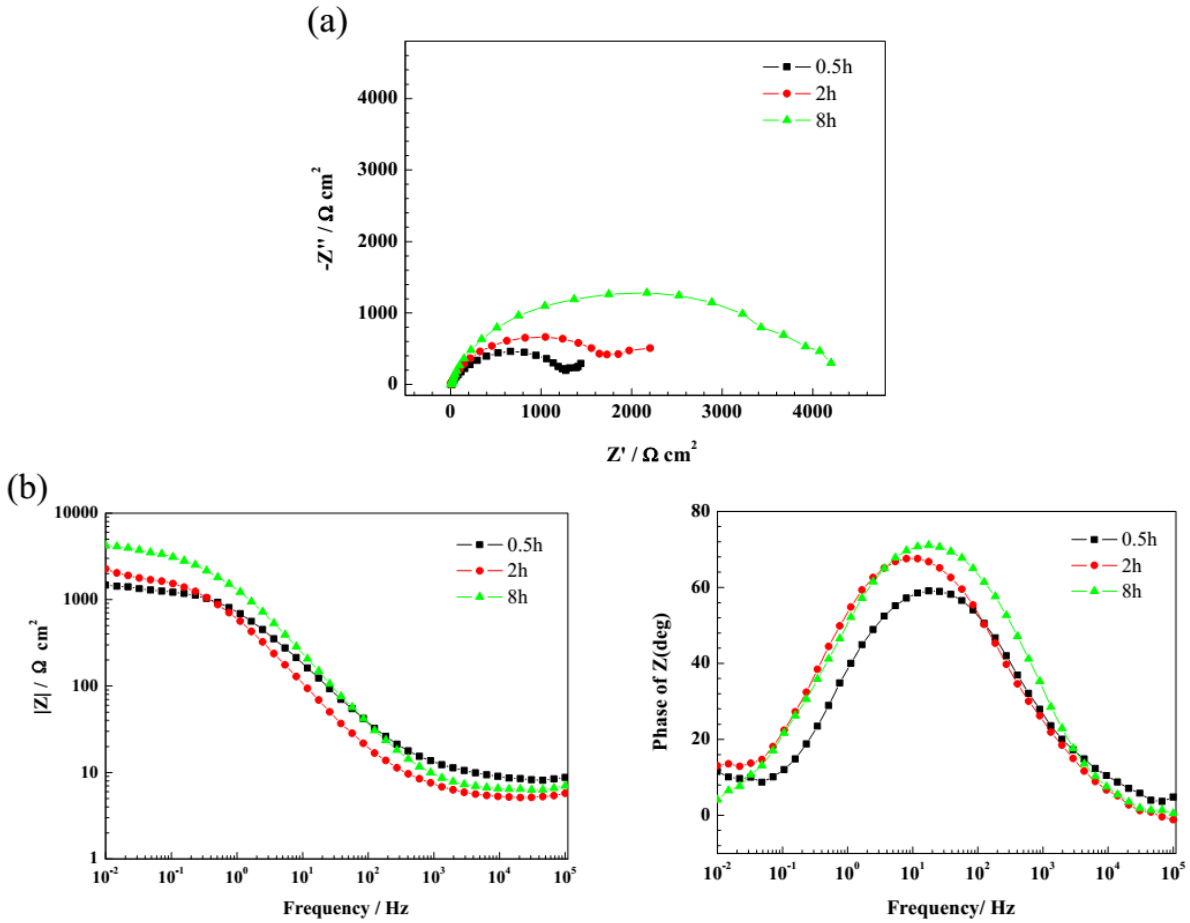

Figure 1. Nyquist (a) and Bode (b) plots of samples in seawater with 1g/L PASP after 0.5 h, 2 h and 8 h immersion, respectively.

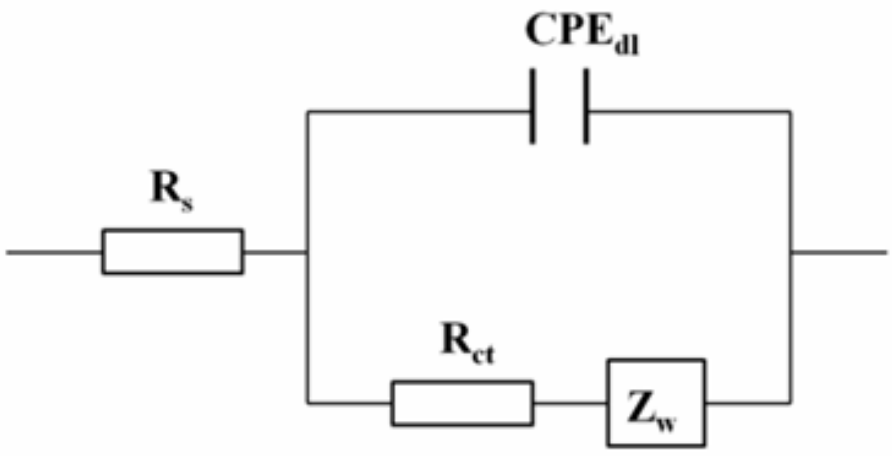

R_s — solution resistance
CPE_{dl} — constant phase element
R_{ct} — charge transfer resistance

Figure 2. Equivalent circuit models used to fit the experiment impedance data of samples in seawater with 1g/L PASP after 8 h immersion.

Table 1. Values of electrochemical impedance parameters in seawater with 1g/L PASP during the 8 h immersion.

Immersion time (h)	R_s (Ω cm^2)	CPE_{dl}		R_{ct} (Ω cm^2)
		Y_{dl} (Ω^{-1}cm^{-2}s^{n}10^{-6})	n_{dl}	
0.5	8.54	249	0.74	1334
2	5.39	341	0.79	1815
8	6.4	142	0.82	3619

The Nyquist and Bode plots of the mild steel in seawater containing 1g/L PASP after different cycles are shown in Fig. 3. The equivalent circuit used to simulate the impedance data is shown in Fig. 4, and the electrochemical parameters are presented in Table 2. It is observed that the value of impedance decreases during the wet/dry cycles and two time constants appear on phase angle in Bode plots. The values of R_{ct} in Table 1 are obviously greater compared to the values of R_{ct} in Table 2, indicating that the inhibition effect of the corrosion process is negligible on the surface of the metal during the cycles. Therefore, the PASP does not play an important role for the protection of mild steel during wet/dry cycles.

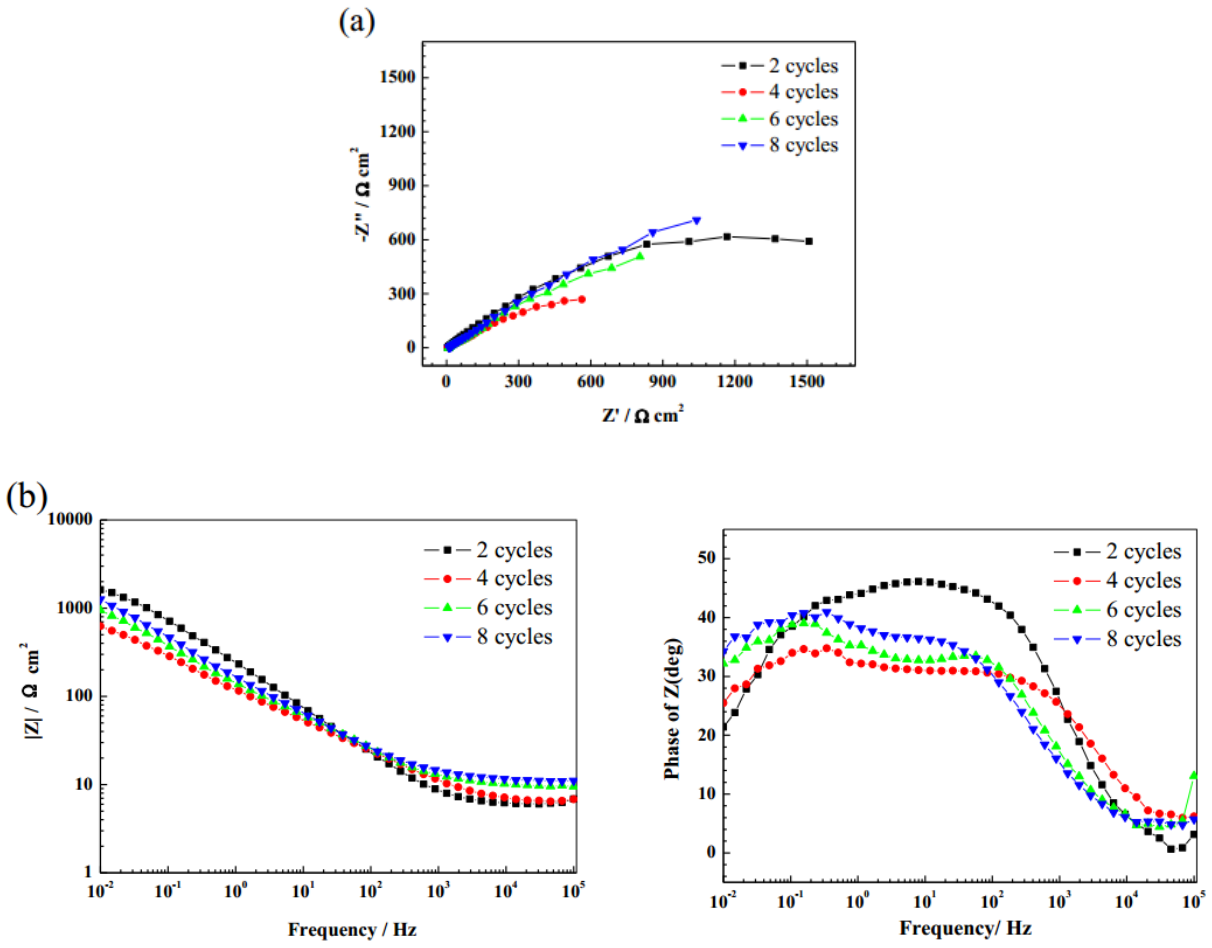

Figure 3. Nyquist (a) and Bode (b) plots of samples in seawater with 1g/L PASP after different cycles.

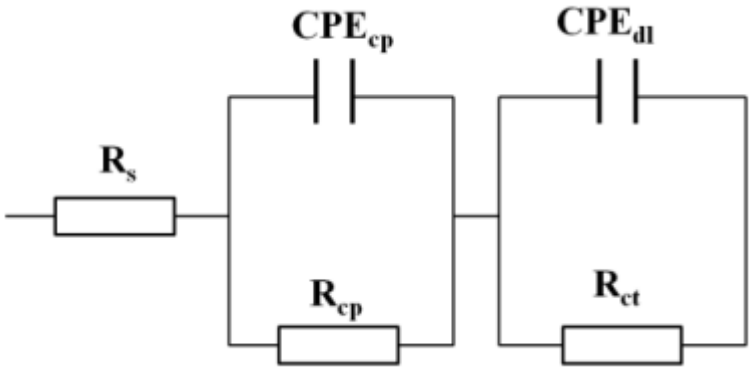

R_s — solution resistance CPE_{dl} — capacitance of double layer
CPE_{cp} — capacitance of corrosion products R_{ct} — charge transfer resistance
R_{cp} — resistance of corrosion products

Figure 4. Equivalent circuit models used to fit the experiment impedance data of samples in seawater with 1g/L PASP during the initial 8 h.

Table 2. Values of electrochemical parameter in seawater with 1g/L PASP after diffenent cycles.

Immersion time	R_s (Ω cm^2)	CPE_{cp}		CPE_{dl}		R_{ct} (Ω cm^2)
		Y_{dl} (Ω^{-1}cm^{-2}s^{n}10^{-6})	n_{cp}	Y_{dl} (Ω^{-1}cm^{-2}s^{n}10^{-6})	n_{dl}	
2 cycles	5.82	1546	0.63	1525	0.68	58.4
4 cycles	5.86	1710	0.59	4128	0.49	13.82
6 cycles	9.15	976	0.77	3295	0.49	32.86
8 cycles	10.45	1634	0.50	1966	0.79	14.68

The Nyquist and Bode plots of the mild steel in seawater containing the mixed inhibitor are shown in Fig. 5. Equivalent circuit is depicted in Fig. 6. The Nyquist spectra show single capacitive loop, indicating that the corrosion was controlled by the charge transfer process.

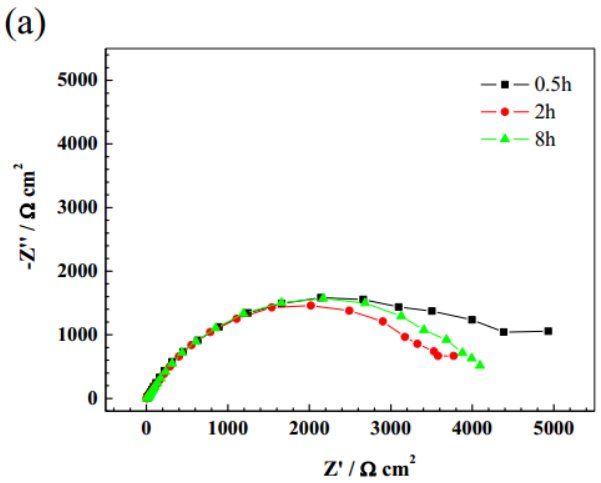

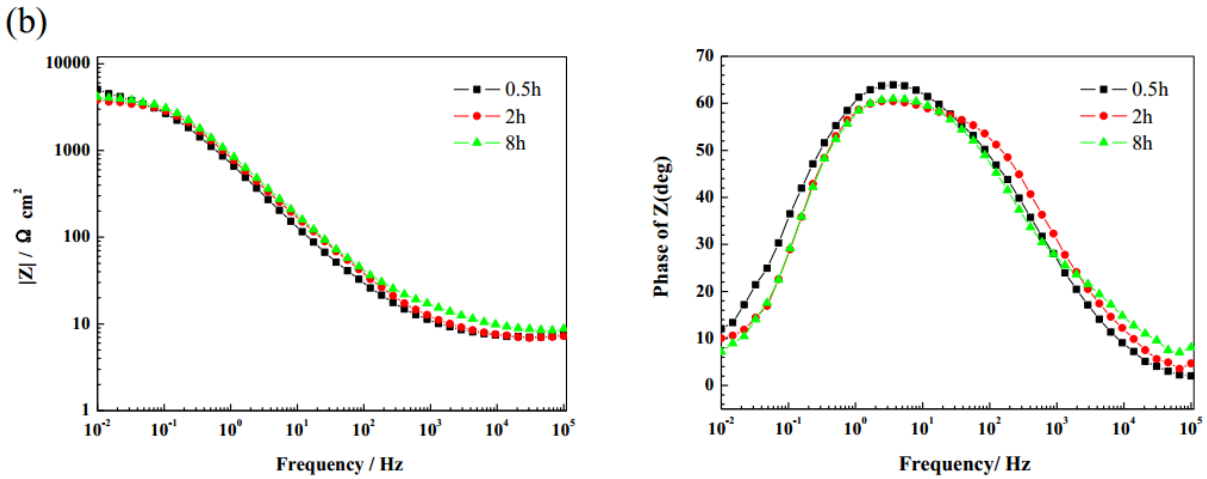

Figure 5. Nyquist (a) and Bode (b) plots of samples in seawater with the mixed inhibitor during the initial 8 h.

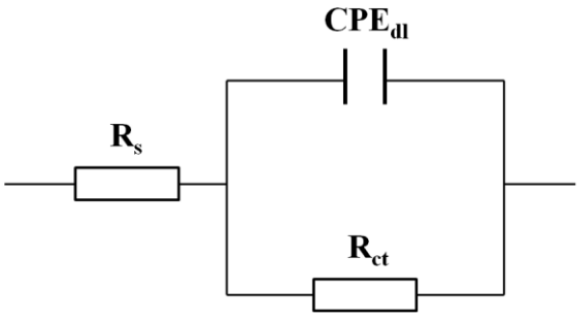

Figure 6. Equivalent circuit models used to fit the experiment impedance data of samples in seawater with the mixed inhibitor during the initial 8 h.

Table 3. Values of electrochemical parameter in seawater with the mixed inhibitor during the initial 8 h.

Immersion time (h)	R_s (Ω cm^2)	CPE_{dl}		R_{ct} (Ω cm^2)
		Y_{dl} (Ω^{-1}cm^{-2}s^{n}10^{-6})	n_{dl}	
0.5	7.2	358	0.73	5312
2	7.0	290	0.71	4379
8	9.4	281	0.70	4879

The change on the diameter of the capacitive loop is negligible with the increase of immersion time, so the formation of the film was almost finished at 0.5 h on the metal surface and the inhibition efficiency is relatively stable. The impedance data are fitted and the electrochemical parameters are given in Table 3. The value of R_{ct} was 4879 Ω cm^2 after the immersion time of 8 h in the mixed inhibitor, compared to 3619 Ω cm^2 in the PASP solutions (see Table 1). Therefore, it can be concluded that the mixed inhibitor has better inhibition efficiency than PASP.

The Nyquist and Bode plots of the mild steel in seawater containing the mixed inhibitor during wet/dry cyclic corrosion tests are shown in Fig. 7.

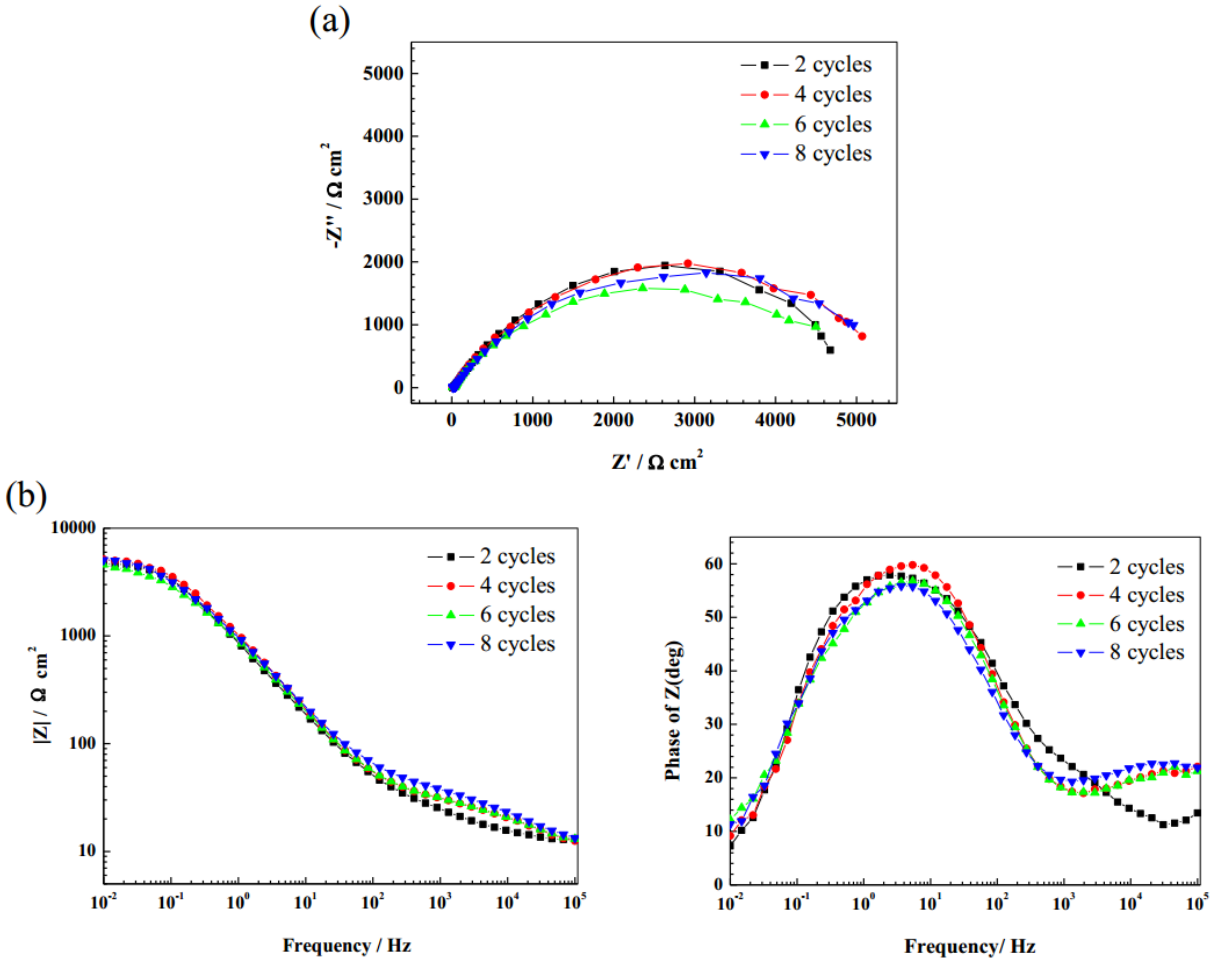

Figure 7. Nyquist (a) and Bode (b) plots of the samples in seawater with the mixed inhibitor after different cycles.

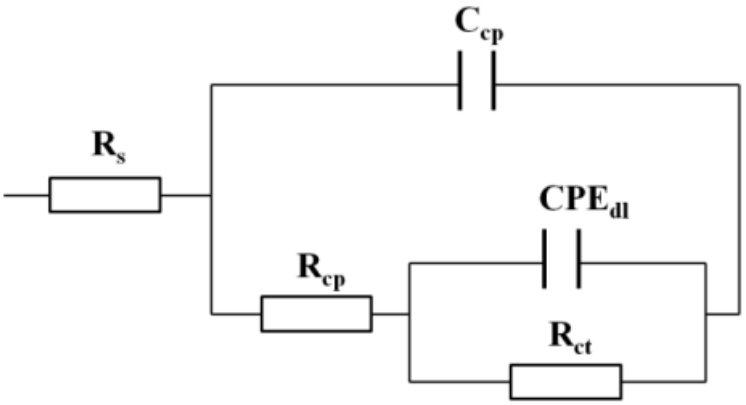

R_s — solution resistance CPE_{dl} — capacitance phase element
C_{cp} — capacitance of corrosion products R_{ct} — charge transfer resistance
R_{cp} — resistance of corrosion products

Figure 8. Equivalent circuit model used to fit the experiment impedance data of samples in seawater with the mixed inhibitor after different cycles.

There are two time constants at the high and low frequency along with the increase of wet/dry cycles. The equivalent circuit shown in Fig. 8 was used to simulate the impedance spectra, and the simulated impedance parameters are shown in Table 4. The R_{ct} value remains stable after several wet/dry cycles, indicating that the mixed inhibitor effectively protects mild steel against corrosion attack during the wet/dry cycles.

Table 4. Values of electrochemical parameter in seawater with the mixed inhibitor after different cycles.

Immersion time	R_s (Ω cm^2)	CPE_{dl}		R_{ct} (Ω cm^2)
		Y_{dl} (Ω^{-1}cm^{-2}s^{n}10^{-6})	n_{dl}	
2 cycles	13.18	277	0.71	5651
4 cycles	11.62	239	0.73	5783
6 cycles	11.74	294	0.69	5138
8 cycles	12.79	275	0.68	5979

3.1.3. Polarization measurements

The polarization curves of mild steel after eight treatments in the wet/dry apparatus are shown in Fig. 9. It reveals that both E_{corr} values in PASP and the mix inhibitors shift to a more negative direction compared to seawater. The addition of PASP and the mix inhibitors has an evident effect on the catholic reaction possibly due to the corrosion products inhibition effect on the oxygen diffusion. The results show that the corrosion current density decreases with the increase of polarization resistance, indicating that both catholic and anodic reaction processes were influenced by corrosion product. Polarization curves of the mixed inhibitor show a passive area from -700 mV to -650 mV, suggesting wolfram element has a protection effect on mild steel due to its weak oxidation. The addition of the mixed inhibitor further reduces cathodic current density in comparison with PASP. The results reveal that zinc ions blocked cathodic reaction.

The related electrochemical parameters are listed in table 5. The inhibition efficiency η value was calculated from polarization measurements according to the following equation (1), where i_{corr} and i^0_{corr} are the corrosion current densities of mild steel without and with the addition of inhibitors in the solution, respectively.

$$\eta(\%) = \left(\frac{i_{corr} - i^0_{corr}}{i_{corr}}\right) \times 100 \quad (1)$$

Table 5 shows that the inhibition efficiency was 72.4% and 92.6% for PASP and the mixed inhibitor, respectively. The results reveal a better inhibitive effect of the mixed inhibitor than PASP alone.

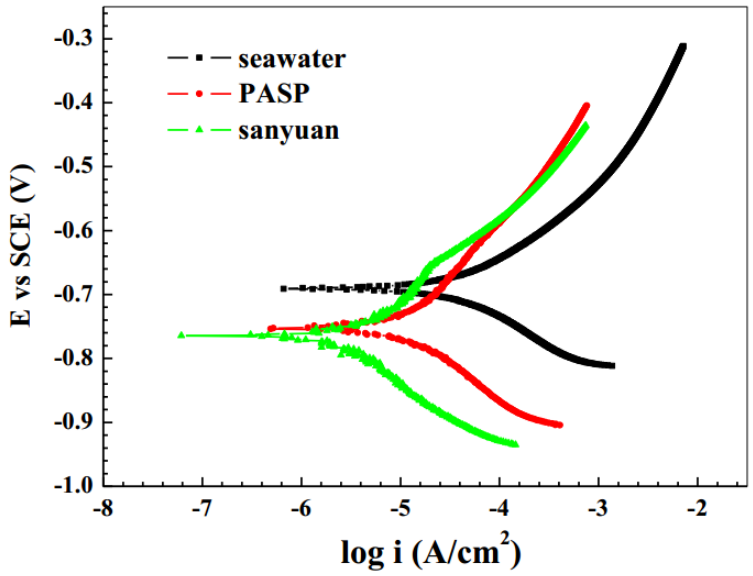

Figure 9. Polarization curves of the samples after 8 cycles in seawater.

Table 5. Polarization curves results and inhibition efficiency of mild steel in seawater, PASP and mixed inhibitor.

Solution	E_{corr}(mV vs SCE)	i_{corr} (μA cm^{-2})	β_a (mV/dec)	β_c (mV/dec)	η_p (%)
Seawater	-688	47.85	113	115	-
PASP	-748	13.19	187	135	72.4
Mixed inhibitor	-722	3.52	145	139	92.6

3.3. Surface analysis

Fig. 10a shows the mild steel surface before the cyclic corrosion tests. The morphology of the sample surface in seawater with PASP after 8 cycles is presented in Fig. 10b. The sample surface was greatly damaged during the wet/dry cyclic tests, as the corrosion products show cluster morphology with some micro-flower structure. The outer layer of the corrosion products is porous and appears uneven and rough, which is strongly adsorbed to the inner layer. In contrast, the single-layer corrosion products on the metal surface immersed in the mixed inhibitor (Fig. 10c) indicate a more protective condition in comparison with that in seawater with PASP (Fig. 10b). A protective layer is formed on the steel surface, which better inhibited corrosion attack due to the inhibitive effect of the mixed inhibitor. These results are in accordance with the inhibition efficiency values presented in Table 5.

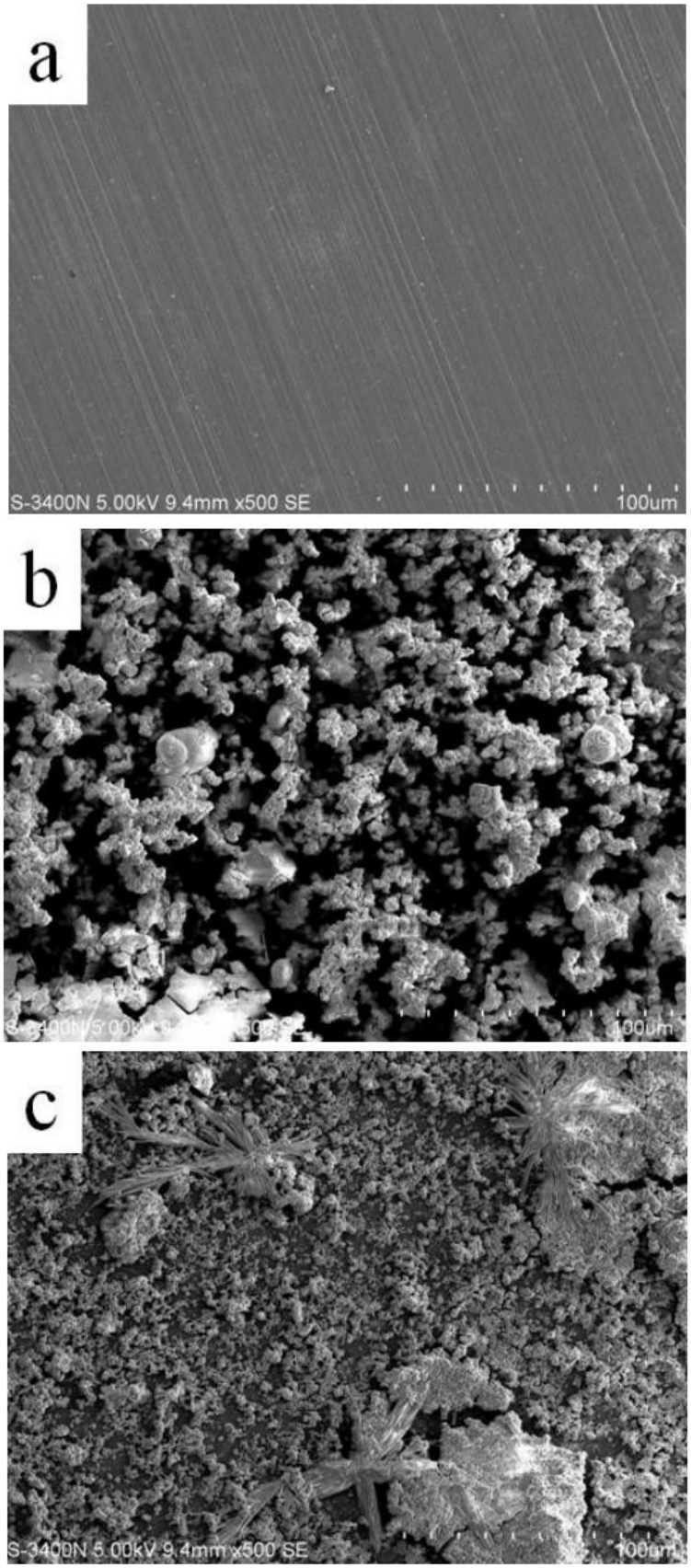

Figure 10. SEM images of sample surface before (a) and after 8 cycles in PASP (b) and the mixed inhibitor (c)

Fig. 11 and Fig. 12 show the XRD patterns of corrosion product powders recorded after 8 cycles in PASP and the mixed inhibitor, respectively. Fig. 11 reveals more oxygen, chloride and magnesium elements but no nitrogen elements, indicating that there are more corrosion products on the surface of mild steel and no PASP absorbed on steel surface. Fig. 12 reveals wolfram, zinc and more ferrum elements on the surface of steel, in which the content of Fe is up to 80%. The results reveal that the mixed inhibitor inhibited the formation of corrosion products on metal surface, and therefore protected the steel against corrosion.

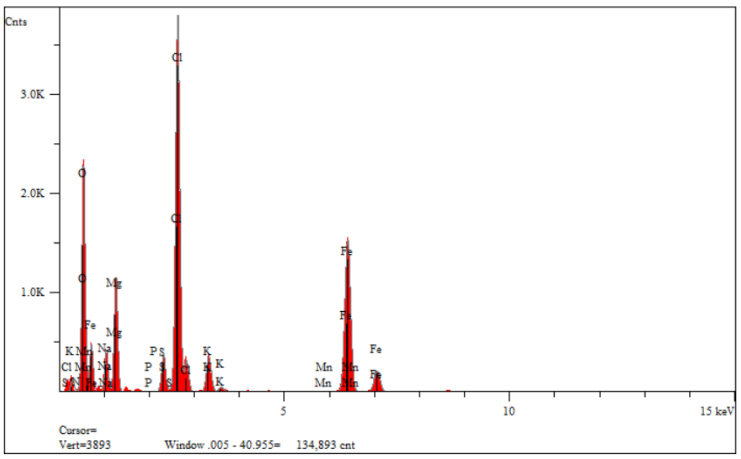

Figure 11. EDS of sample surface after 8 cycles in seawater with PASP.

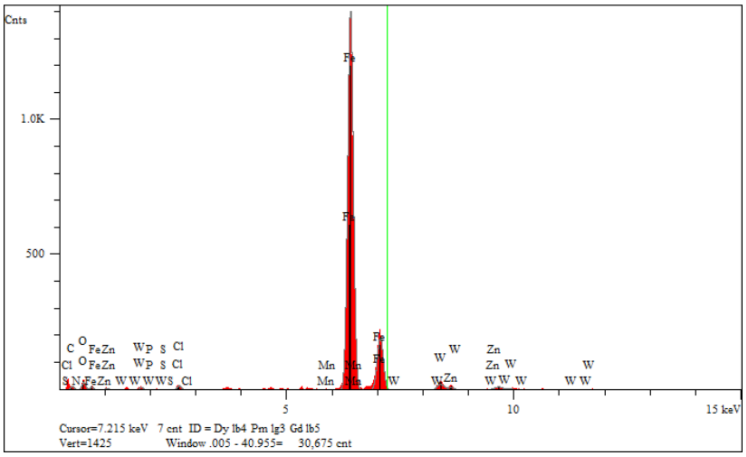

Figure 12. EDS of sample surface after 8 cycles in seawater with the mixed inhibitor.

The FTIR patterns of corrosion products measured after 8 cycles in seawater with PASP are presented in Fig. 13a. An absorption band appears at the vicinity of 1020 cm^{-1}, which is the major band of lepidocrocite [24, 25]. The absorption band at 3411cm^{-1}, 1652cm^{-1}, 1509cm^{-1} and 1390cm^{-1} corresponds to polyaspartic acid[26, 27]. The observation of corrosion products containing γ-FeOOH indicates that polyaspartic acid was absorbed on the metal surface. Fig. 13b shows the FTIR spectra of corrosion products measured after 8 cycles in seawater with the mixed inhibitor. The absorption bands

at 3411cm^{-1}, 1652cm^{-1}, 1509cm^{-1} and 1390cm^{-1} are related to the existence of polyaspartic acid. The absorption band between 1020 cm^{-1} and 1128 cm^{-1} is assigned to the existence of lepidocrocite.

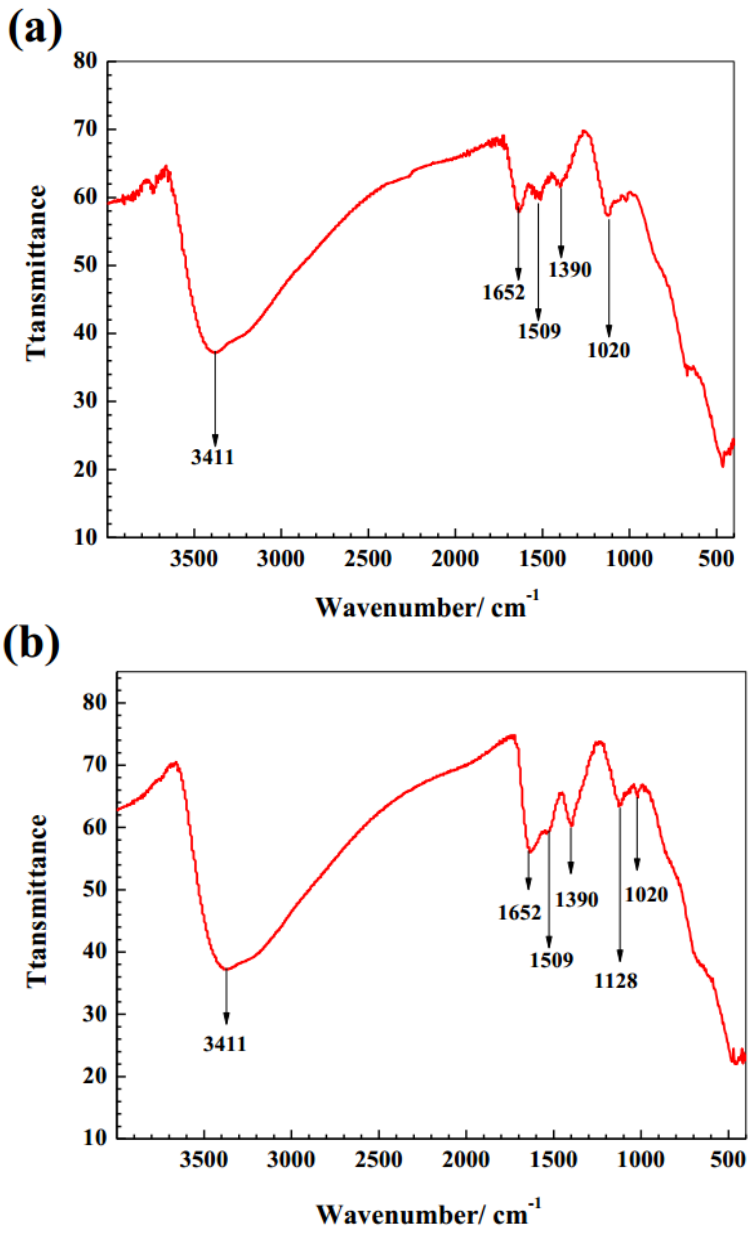

Figure 13. FTIR patterns of the corrosion products in seawater with (a) PASP and (b) the mixed inhibitor.

Fig. 14 shows the XRD patterns of corrosion product powders measured in seawater with PASP and the mixed inhibitor. Fig. 14a only reveals mainly green rust and γ-FeOOH peaks while Fig. 14b reveals mainly green rust, γ-FeOOH and β-FeOOH peaks.

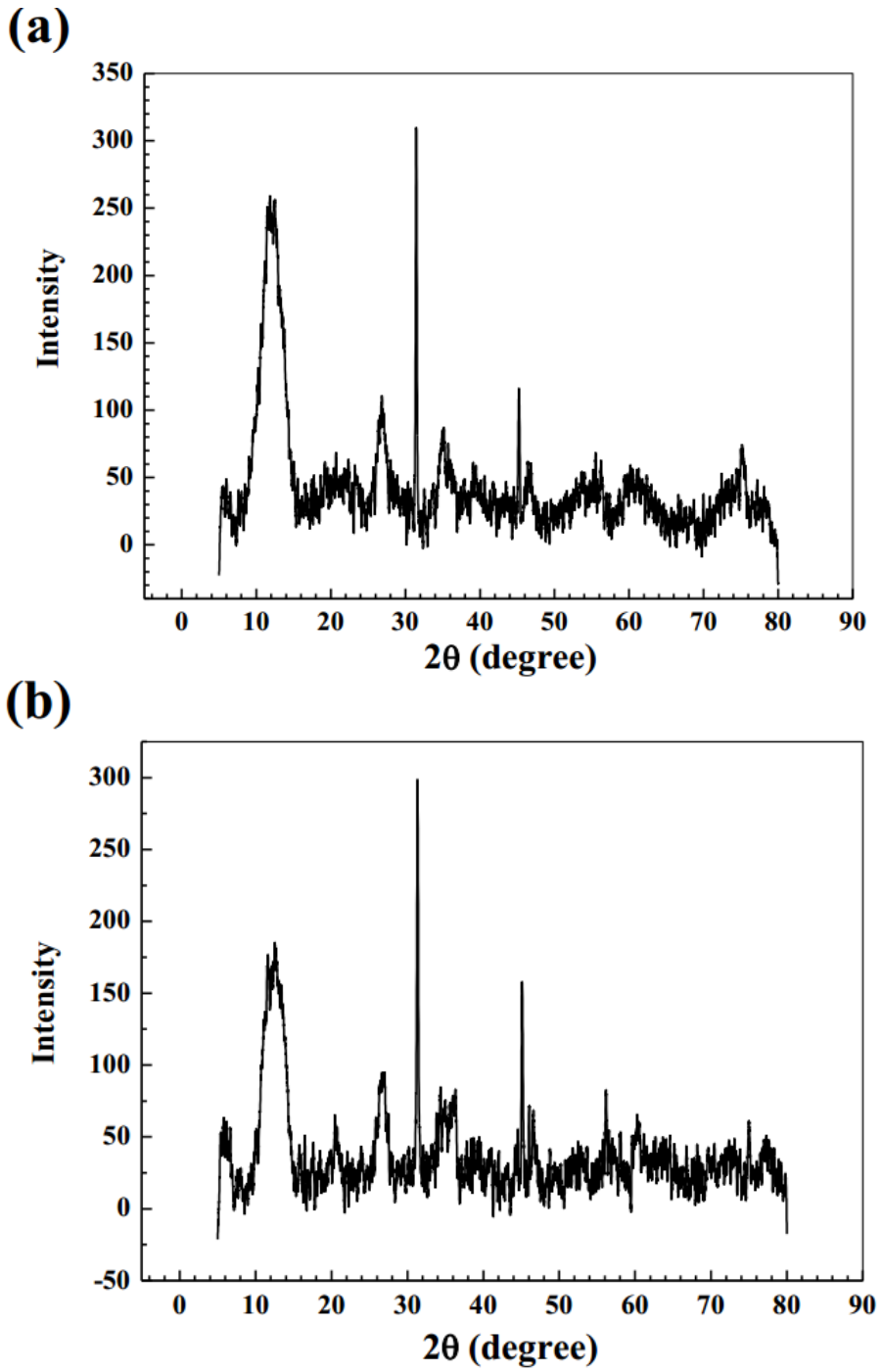

Figure 14. XRD patterns of the corrosion products in seawater with (a) PASP and (b) the mixed inhibitor.

4. CONCLUSION

The corrosion of mild steel under seawater wet/dry cyclic condition is inhibited effectively by the mixed inhibitor. The value of the inhibition efficiency was 92.6% in the seawater with the mixed inhibitor compared to 72.4% with PASP.

Different morphologies were observed on the surface of steels with the PASP and the mixed inhibitor. The corrosion product layer formed in the mixed inhibitor is more protective.

EDS analysis reveals that the corrosion products contain wolfram, zinc and more ferrum elements with the mixed inhibitor, indicating less corrosion products and less corrosion attack.

The results of FTTR spectra indicate that PASP absorbed on the steel surface both in seawater with PASP and the mixed inhibitor after wet/dry cycles.

ACKNOWLEDGEMENT
The authors wish to acknowledge National Basic Research Program of China（No.2014CB643304）.

References

1. N. M'hiri, D. Veys-Renaux, E. Roccab, I. Ioannou, N. Boudhrioua and M. Ghoul, *Corros. Sci.*, 102 (2016) 55.
2. B. Qian, B. Hou and M. Zheng, *Corros. Sci.*, 72 (2013) 1.
3. B. Qian, J. Wang, M. Zheng and B. Hou, *Corros. Sci.*, 75 (2013) 184.
4. K. Ansari, M. Quraishi and A. Singh, *Corros. Sci.*, 95 (2015) 62.
5. A. Ghazi, E. Ghasemi , M. Mahdavian , B. Ramezanzadeh and M. Rostami, *Corros. Sci.*, 94 (2015) 207.
6. H. Vakili, B. Ramezanzadeh and R. Amini, *Corros. Sci.*, 94 (2015) 466.
7. J. Zhang, X. Gong, H. Yu and M. Du, *Corros. Sci.*, 53(2011) 3324.
8. S. Nataraja, T. Venkatesha, K. Manjunatha, B. Poojary, M. Pavithra and H. Tandon, *Corros. Sci.*, 53 (2011) 2651.
9. B.Zhang, C. He, C. Wang, P. Sun, F. Li and Y. Lin, *Corros. Sci.*, 94 (2015) 6.
10. K. Zhang, B. Xu, W. Yang, X. Yin, Y. Liu and Y. Chen, *Corros. Sci.*, 90 (2015) 284.
11. S. Umoren, Y. Li and F. Wang, *Corros. Sci.*, 52 (2010) 2422.
12. M. Deyab and S. Abd El-Rehim, *Corros. Sci.*, 65 (2012) 309.
13. S. Umoren, O. Ogbobe, I. Igwe and E. Ebenso, *Corros. Sci.*, 50 (2008) 1998.
14. B. Zhang, C. He, X. Chen, Z. Tian and F. Li, *Corros. Sci.*, 90 (2015) 585.
15. F. Liu, L. Zhang, X. Yan, X. Lu, Y.Gao and C. Zhao, *Corros. Sci.*, 93 (2015) 293.
16. V. Shinde and P. Patil, *Electrochim. Acta.*, 78 (2012) 483.
17. X. Wang, B. Lee and L. Mann, *Colloids Surf.*, A 202 (2002) 71.
18. M. Tomida, T. Nakato, S. Matsunami and T. Kakuchi, *Polym.* ,38 (1997) 4733.
19. S. Wolk, G. Swift, Y. Paik, K. Yocom, R. Smith and E. Simon, *Macromolecules*, 27 (1994) 7613.
20. Y. Liu, C. Liu and N. Gu, *Sichuan Environ.*, 32 (2014)11.
21. X. Li, S. Deng, H. Fu and G. Mu, *Corros. Sci.*, 52 (2010) 1167.
22. Q. Xu and S. Huang, *J. Shanghai Univ. Electr. Power*, 22 (2006) 71.
23. R. He, P. Du, C. Li and N. Gu, *Corros. Prot.*, 33 (2012) 761.
24. N. Sasrazadani, *Corros. Sci.*, 39 (1997) 1845.
25. S. Hug and D. Bahnemann, *J. Electron Spectrosc.*, 150 (2006) 208.
26. G. Ma, Q. Yang, F. Ran, Z. Dong and Z. Lei, *Appl. Clay Sci.*, 118 (2015) 21.
27. Y. Gao, L. Fan, L. Ward and Z. Liu. *Desalination*, 365 (2015) 220.